Asymmetry Requirements in the Photosynthetic Reaction Center of *Rhodobacter capsulatus*†

Aileen K. W. Taguchi, J. Elizabeth Eastman, Dennis M. Gallo, Jr.,‡ Eric Sheagley, Weizhong Xiao,§ and Neal W. Woodbury*

Department of Chemistry and Biochemistry and the Center for the Study of Early Events in Photosynthesis, Arizona State University, Tempe, Arizona 85287-1604

Received September 13, 1995; Revised Manuscript Received January 3, 1996⊗

ABSTRACT: Nine large-scale symmetry reaction center mutants were constructed in *Rhodobacter capsulatus* by replacing segments of the M subunit gene with the homologous region of the L subunit gene. Between them, the mutations resulted in symmetrization of essentially the entire region from the carboxy terminal portion of the C helix through most of the E helix. The amino acids in this region define about 80% of the environment of the reaction center cofactors. These studies show that roughly 80% of the amino acids that come in close contact with the cofactors involved in initial electron transfer can be made symmetric in a piecewise manner without loss of the ability to grow photoheterotrophically. However, the amino acid regions near the quinones and iron atom are much more sensitive to symmetrization and most of the large-scale changes in this region resulted in the loss of photosynthetic viability, probably due to loss of stable reaction centers from the photosynthetic membrane. More detailed analysis of the isolated photosynthetic membranes from these mutants showed that in all cases but one, there was some amount of charge separation occurring in the mutant reaction centers. This bank of mutants serves as a useful starting point for more detailed studies of the differential molecular interactions which occur between the two reaction center subunits and their associated cofactors.

One of the most intriguing aspects of the three-dimensional crystal structure of the photosynthetic reaction center from purple nonsulfur bacteria is the approximate 2-fold axis of symmetry that relates the L and M subunits and their associated cofactors (Deisenhofer et al., 1984; Allen et al., 1987; Chang et al., 1991; Ermler et al., 1994). This symmetry results in two potential pathways for electron transfer in the reaction center, beginning with a bacteriochlorophyll dimer, P,[1] near the periplasmic side of the reaction center. The dimer is flanked by two symmetrically placed monomer bacteriochlorophylls, B_A and B_B, each of which is followed by a monomer bacteriopheophytin, H_A and H_B, and finally by two quinones, Q_A and Q_B, near the cytoplasm. Despite this structural symmetry, light-induced charge separation appears to occur almost exclusively along the A side cofactors [for reviews see Kirmaier and Holten (1987, 1993), Feher et al. (1989), Parson (1991), Martin and Vos (1992), Zinth and Kaiser (1993), and Woodbury and Allen (1995); previous measurements of charge separation asymmetry are discussed in more detail in the following paper in this issue, Lin et al. (1996)].

There are several differences between the A and B branches that could result in electron transfer asymmetry. There is a carotenoid within 4 Å of B_B in wild type *Rhodobacter sphaeroides*, but there is no corresponding carotenoid on the A side (Yeates et al., 1988). However, this carotenoid is not present in the R-26 strain of *Rb. sphaeroides*, and high-resolution measurements of electron transfer directionality on the picosecond time scale have shown no detectable electron transfer to H_B in this strain (Kirmaier et al., 1985; Lockhart et al., 1990). Another source of asymmetry in the reaction center is the H subunit. The interaction between H and the LM core is asymmetric relative to the axis of approximate rotational symmetry. However, the H subunit does not come in close contact with the redox active cofactors making H a less likely source of electron transfer asymmetry. This leaves the asymmetry in amino acid identity between the L and M subunits which gives rise both to small but significant differences in the orientation of the redox active cofactors on the A and B sides of the reaction center (Feher et al., 1989) and to differences in the static fields [e.g., Parson et al. (1990), and Gehlen et al. (1994)] and the dielectric properties (Steffen et al., 1994) of the two potential electron transfer branches.

The L and M subunits in *Rb. sphaeroides* share only about one-third of their amino acid residues in common (Williams et al., 1984), even though their overall three-dimensional structures are quite similar (Deisenhofer et al., 1984; Allen et al., 1987; Chang et al., 1991; Ermler et al., 1994). It is possible to replace sections of the gene for either the L or M subunit with nucleotide sequences from the other and to express partially symmetrized reaction centers (Robles et al.,

† This work was supported by grants DMB 91-58251, MCB 9219378, and MCB 9404925 from the National Science Foundation. Instrumentation was purchased with funds from NSF Grant DIR-8804992 and Department of Energy grants DE-FG-05-88-ER75443 and DE-FG-05-87-ER75361. This is Publication No. 259 from the Arizona State University Center for the Study of Early Events in Photosynthesis.

* To whom correspondence should be addressed.

‡ Present address: Department of Chemistry, Wallberg Hall, Augustana College, Rock Island, IL 61201.

§ Present address: Department of Pathology and Laboratory Medicine, Hospital of University of Pennsylvania, 7−114 Founders, 3400 Spruce St., Philadelphia, PA 19104.

⊗ Abstract published in *Advance ACS Abstracts,* February 15, 1996.

[1] Abbreviations: *Rb.*, *Rhodobacter*; *Rp.*, *Rhodopseudomonas*; P, bacteriochlorophyll dimer; B, monomer bacteriochlorophyll; H, monomer bacteriopheophytin; Q, quinone; wt, wild type; NMP, *N*-methylprotoporphyrin.

0006-2960/96/0435-3175$12.00/0

Table 1: *Rhodobacter capsulatus* Strains

strain	description[a]	reference
U43	Spec^r::Δpuf$\beta\alpha$LMX LHII$^-$	Youvan et al. (1985)
ΔRC6	Kan^r::Δpuf$\beta\alpha$LMX LHII$^+$	Chen et al. (1988)

[a] Spec, spectinomycin; Kan, kanamycin; Δ, deletion.

1990; Taguchi et al., 1992; Stocker et al., 1992; Coleman & Youvan, 1993). In this report, we describe nine new large-scale mutations which increase the protein symmetry surrounding the redox active cofactors. As in the *sym1* mutation of *Rb. capsulatus* described previously (Taguchi et al., 1992), the M side protein sequence was replaced with symmetry-related L protein sequence in a step-wise fashion. Taken together, these mutations result in symmetrization of about 80% of the M subunit amino acids that come in close contact with cofactors potentially involved in electron transfer in the reaction center.

EXPERIMENTAL PROCEDURES

Strains. The *Rb. capsulatus* background strains, U43 and ΔRC6, were used for expression of the plasmid encoded *puf* operon in the presence (ΔRC6) or absence (U43) of the LHII (light harvesting II) antenna (see Table 1).

Plasmid Construction. Seven unique restriction enzyme sites were utilized to introduce *pufL* gene sequences into cloned *pufM* gene sequences via cassette mutagenesis as described for the s*ym1* mutation (Taguchi et al., 1992). The sites were *Nar*I (around nucleotide M487), *Xmn*I (M559), *Pvu*I (M614), *Bst*EII (M675), *Sac*II (M720), *Nco*I (M781), and *Bam*HI (M847). Nine large-scale *sym* mutations were constructed containing replacement regions ranging from 5 to 23 amino acids. Annealed double-stranded oligonucleotides were initially cloned into either pBRM-N1 or pBSM and subcloned into the pCR expression vector as described previously (Taguchi et al., 1992). pBRM-N1 has been described previously (Taguchi et al., 1992) as a derivative of pBR322 containing a *Kpn*I−*Bam*HI fragment of *puf*M. The plasmid pBSM was constructed from the same *Kpn*I−*Bam*HI fragment subcloned into pBS$^-$ (Stratagene). Each pBRM-N1 and pBSM construct was sequenced through the region of interest.

The nine mutations combined resulted in the replacement of 113 of the 119 amino acids from M162 through M280 by their *pufL* analogs. The specific replacement sequences are shown in Figure 2 for the mutations *sym0*, *sym1*−*1*, *sym1*−*2*, *sym2*−*1*, *sym2*−*2*, *sym3*, *sym4*, *sym5*−*1*, and *sym5*−*2*. Figure 1 diagrams the corresponding regions of the reaction center on the basis of the X-ray crystal structures of *Rp. viridis* and *Rb. sphaeroides* reaction centers (Deisenhofer et al., 1984; Allen et al., 1987; Chang et al., 1991; Ermler et al., 1994). Mutations *sym1*−*1* and *sym1*−*2* are subsets of a previously described mutation, *sym1* (Taguchi et al., 1992).

Oligonucleotides for cassette mutagenesis were designed by replacing *pufM* sequences with analogous sequence from *pufL*, but maintaining the sticky ends required for ligation. A few silent mutations were engineered in for ease of screening. These were nucleotides M516(T), M519(A), M579(C), M564(T), M616(T), M617(C), M618(G), M672(C), and M840(A). Seven amino acids between M162 and M280 which were not replaced are listed in the Results section.

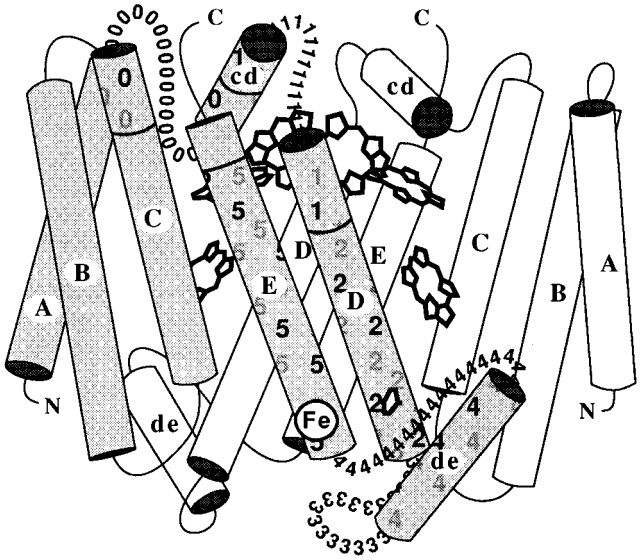

FIGURE 1: Diagrammatic representation of the structure of the photosynthetic reaction center showing the approximate relationships between the cofactors and the different regions of the L and M subunits. The tubes represent α-helices. The numbers on the tubes, or forming the strands connecting the tubes, denote the protein regions mutated in this work. The region covered by zeroes corresponds to the *sym0* region; that covered by ones corresponds to the *sym1* region, etc. The information to generate this diagrammatic representation was taken from the X-ray crystal structures of *Rb. sphaeroides* and *Rp. viridis* (Deisenhofer et al., 1984; Allen et al., 1987; Chang et al., 1991; Ermler et al., 1994) and is based on a very similar representation of the *Rp. viridis* structure from Michel and Deisenhofer (1988).

U43(pCR) was employed as the wild type (Youvan et al., 1985; Taguchi et al., 1993). U43 is a deletion background lacking most of the genomic *puf* operon sequences. Plasmid pCR contains an intact *puf* operon coding for the native reaction center and antenna proteins, and can be conjugated from *Escherichia coli* into *Rb. capsulatus*. U43(pΔM) was used as the negative control. Plasmid pΔM is similar to pCR except that an 0.8 kb *Sal*I fragment has been deleted from the 0.9 kb coding sequence of the *puf*M gene.

Photosynthetic Growth Assays. The photosynthetic growth assay on plates was done under strictly anaerobic conditions essentially as described by Taguchi et al. (1992).

Suppressor Analysis. MPYe overnight cultures (5 mL or diluted to 5 mL) were gently mixed with 5 mL of 42 °C MPYe + 1.5% agar + 10 μg of kanamycin/mL in 17 × 100 mm clear polycarbonate culture tubes and incubated at 32 °C under illumination (Taguchi et al., 1993).

Growth of Rb. capsulatus and Isolation of Chromatophores and Reaction Centers. All *Rb. capsulatus* strains were grown in RCVPY medium (Xiao et al., 1994). Cells were harvested by centrifugation and broken in a French press at 20 000 psi. Chromatophores were isolated by differential centrifugation essentially as described by Prince and Youvan (1987) as modified by Xiao et al. (1994).

When possible, reaction centers were isolated from membranes by solubilization and column chromatography (Taguchi et al., 1992). Spectral measurements of reaction centers were performed in 10 mM KPO_4 (pH 7.35), 0.05% LDAO, except for measurements with quinones reduced. In this case, the LDAO buffer was replaced by 10 mM KPO_4 buffer (pH 7.35), 0.04% Triton X-100 to avoid precipitation of LDAO under reducing conditions. This was accomplished by binding reaction centers to a DEAE-Sephacel (Pharmacia)

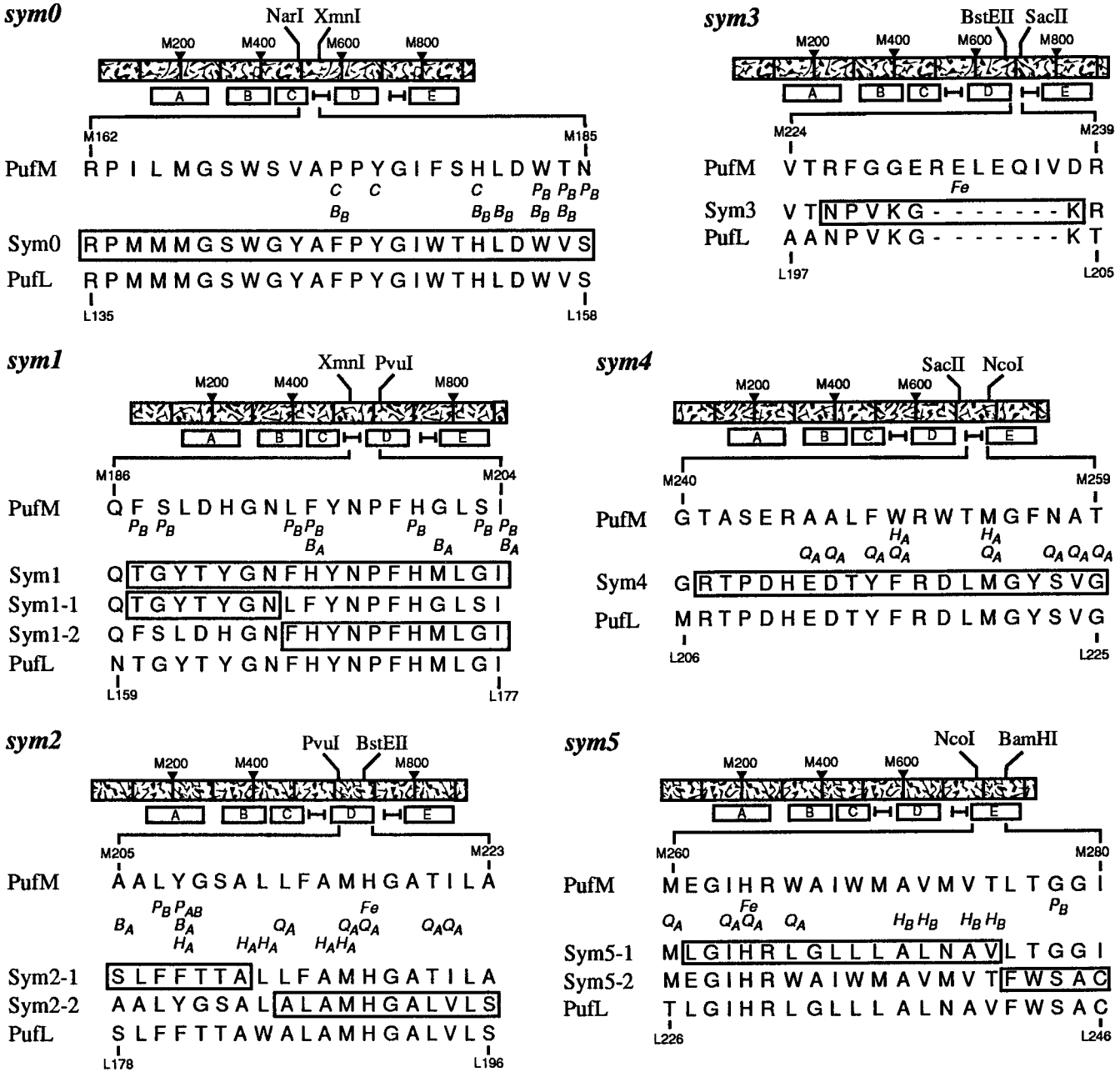

FIGURE 2: Each of the six panels represents a *sym* region of the *Rb. capsulatus* reaction center showing the mutated amino acid sequences compared to the sequence of the L and M subunits of *Rb. capsulatus* in the same region. The DNA sequence of the *pufM* gene is represented by the long mezzotinted rectangle with nucleotide positions indicated at about 200 base intervals. The locations of the α-helices in the *pufM* gene product as determined from the *Rb. sphaeroides* X-ray structure (Allen et al., 1987; Chang et al., 1991; Ermler et al., 1994) are shown below the gene. The amino acid sequences for the PufM, Sym, and PufL proteins are shown in the lower part of each panel applying the alignment of Michel et al. (1986). Cofactors which appear within 4.0 Å of a particular M subunit residue in the *Rb. sphaeroides* structure are shown below the *Rb. capsulatus* M subunit sequence in each panel. Distance information was compiled from Allen et al. (1988), Komiya et al. (1988), Yeates et al. (1988), and El-Kabbani et al. (1991).

column at low ionic strength, washing with 10 column volumes of the Triton X-100 buffer, and then eluting with the same buffer plus 300 mM KCl. This was then dialyzed and concentrated using a Centricon-30 centrifugal filtration unit (Amicon). Wild type reaction centers isolated in this way contain the normal complement of bacteriochlorophylls, bacteriopheophytins, and a carotenoid, as determined by HPLC analyses of extracts (Gallo, 1994). However, Q_B is almost completely missing, as assayed by the lifetime of the recombination reaction after a short flash (Taguchi et al., 1992).

Protein Analyses. Protein levels in chromatophore preparations were assayed using a modification of the original Lowry protein assay (Peterson, 1977). SDS gel electrophoresis of chromatophore samples was carried out as described by Zilsel et al. (1989).

Spectroscopic Analyses. Ground state absorbance spectra and light-minus-dark difference absorbance spectra were performed as described in Woodbury et al. (1995). For all of the $P^+Q_A^-$ spectra, the OD_{875} was the same for each sample and the signal size in the 800 nm region was linearly dependent on actinic light intensity.

Fluorescence decay measurements of reaction centers and chromatophores were performed using time-correlated single-photon counting (Taguchi et al., 1992). Emission was collected in 2000 time channels each 5 ps in width. All

fluorescence measurements were performed with quinones reduced by the addition of dithionite (5 mM for reaction centers in the Triton X-100 buffer described above and 10 mM for chromatophores). The optical density of the sample was approximately 0.15 in a 1.5 mm pathlength cell at the wavelength of excitation (860 nm).

Measurement of P/P$^+$ Midpoint Potentials. Chemical titrations of the P/P$^+$ midpoint potential were performed essentially as described in Murchison et al. (1993). Electrochemical titration of midpoint potentials was performed in collaboration with Drs. Nagarajan and Parson at the University of Washington in Seattle essentially as described in Nagarajan et al. (1993). Since some mutations were more stable during the extended titrations under conditions of high ionic strength, all chemical and electrochemical titrations were performed with a KCl concentration of 280−300 mM. For wild type, changing the KCl concentration from 300 to 20 mM had essentially no effect on the measured P/P$^+$ potential. However, a significant effect of salt concentration both on the P/P$^+$ potential and on the reaction center spectrum was seen with *sym2−1*. The details of this salt dependence will be published elsewhere.

RESULTS

Seven unique restriction enzyme sites spanning the 3′ half of the *puf*M gene were utilized to construct nine large-scale *sym* mutations. Including the previously described *sym1* mutant (Taguchi et al., 1992), the total region of mutation extends from the carboxy terminal portion of the C helix of PufM (M162) through most of the E helix (M280). These regions encompass about 80% of the M subunit amino acid residues which come in close contact with the reaction center cofactors. Gln(M186), Val(M224), Thr(M225), Arg(M239), Gly(M240), and Met(M260) were not replaced by their PufL analogs due to their positions within restriction enzyme recognition sites. In addition, Leu(M212) was not replaced by Trp since the reversion analysis of Robles and colleagues (1990) suggested that such a change would result in loss of H_A and reaction center activity.

The nine *sym* mutations are described in Figures 1 and 2. The *sym1* region which contains *sym1−1* and *sym1−2* was also described previously (Taguchi et al., 1992). Each *sym* mutation was expressed from a plasmid in the Puf$^-$ *Rhodobacter capsulatus* deletion strain, U43.

Photosynthetic Growth Assays of the Symmetry Mutants. Photosynthetic ability was tested on plates in an anaerobic chamber (see Experimental Procedures). The *sym1* (Taguchi et al., 1992), *sym1−1*, *sym1−2*, *sym2−1*, *sym5−1*, and *sym5−2* mutant strains all showed photosynthetic growth capability by the criterion that a statistically equivalent number of colonies grew on anaerobically grown plates in the light for 13 days as on aerobically grown plates in the dark. Barely visible microcolonies were seen for the negative control (ΔM), *sym2−2*, *sym3*, and *sym4* mutant strains under photosynthetic growth conditions. No colonies grew on plates grown anaerobically in the dark. On the basis of the time of initial appearance of photosynthetic growth, one can roughly order the strains from most vigorous photosynthetic growth to least: (wt) > (*sym1−1*, *sym1−2*, *sym2−1*, *sym5−2*) > (*sym1*, *sym5−1*). The mutants *sym0*, *sym2−2*, *sym3*, and *sym4* showed no growth above the negative control (Table 2).

Table 2: General Characteristics of the *sym* Mutants

genotype	PS[a]	A_{875}/g[b]	τ_A[c] (ps)	τ_D[d] (ns)	P$^+$Q$^-$ [e]	PAGE[f]
wt	+++	590	42	7.8	++	++
ΔM	−	45	780		−	−
sym0	−	81	190	6.9	+	−
sym1	+	500	98	1.3	++	++
sym1−1	++	450	68	8.9	++	++
sym1−2	++	920	71	1.3	++	++
sym2−1	++	350	280	4.3	++	++
sym2−2	−	100	470	4.0	+	−
sym3	−	100	400	3.7	+	−
sym4	−	80	840		−	−
sym5−1	+	94	110	6.5	+	+
sym5−2	++	300	59	8.2	++	++

[a] "+++", very photosynthetically active; "−", not photosynthetically viable. [b] Absorbance at 875 nm of a chromatophore sample divided by grams of total protein. [c] Overall fluorescence decay time of the antenna defined as the total integrated fluorescence divided by the total initial amplitude of the fluorescence. [d] Decay time of the longest lived fluorescence component. [e] P$^+$Q$^-$ signal near 800 nm: "++" is the largest absorbance change, "−" means no detectable signal. Data taken from Figure 3. [f] Presence of reaction center H subunit assayed by polyacrylamide gel electrophoresis.

SDS−PAGE Analysis of Chromatophore Proteins. Chromatophores were solubilized in SDS, subjected to sodium dodecyl sulfate polyacrylamide gel electrophoresis (SDS−PAGE), and Coomassie stained. The most easily visualized reaction center band by this method is the H subunit. An H subunit band was clearly present at approximately 30 kDa on the gel for *sym1*, *sym1−1*, *sym1−2*, *sym2−1*, and *sym5−2* and faintly present in *sym5−1*. It could not be discerned above the background in *sym0*, *sym2−2*, *sym3*, and *sym4* (summarized in Table 2).

Ability of sym Mutant Reaction Centers to Trap Antenna Excitation in Chromatophores. Time-correlated single-photon counting was employed to measure the decay of the antenna excited singlet state. The fluorescence decays at 900 nm are shown in Figure 3 for chromatophore samples from the wild type, each of the nine *sym* mutants, and the ΔM deletion mutant. Note that the log of the fluorescence is plotted as a function of time in this figure. For wild type, the bulk of the fluorescence decays within 100 ps, leaving a small amount of residual fluorescence which lives for many nanoseconds. The initial decay represents the trapping of the antenna excited state by the reaction center. The long-lived fluorescence has been interpreted as back electron transfer from the charge-separated state P$^+$H$_A^-$ reforming the antenna excited state (Woodbury & Parson, 1986, and references therein) and has a lifetime comparable with that of the P$^+$H$_A^-$ state in isolated reaction centers (Schenck et al., 1982). In the M subunit deletion strain, ΔM, the initial fluorescence decay is much slower, presumably representing the overall decay of the antenna fluorescence in the absence of active reaction centers. Note that there is no fluorescence which persists on the many nanosecond time scale in the deletion strain, since no P$^+$H$_A^-$ is formed. The other mutants lie between these two extremes.

Even in the case of the M subunit deletion mutant, which presumably has no active reaction centers, an exponential decay analysis of the fluorescence decay requires at least two exponential decay components of a few hundred ps and about 800 ps, the latter dominating the decay. None of the mutations with active reaction centers (including the wild type) can be described accurately by two exponential decay

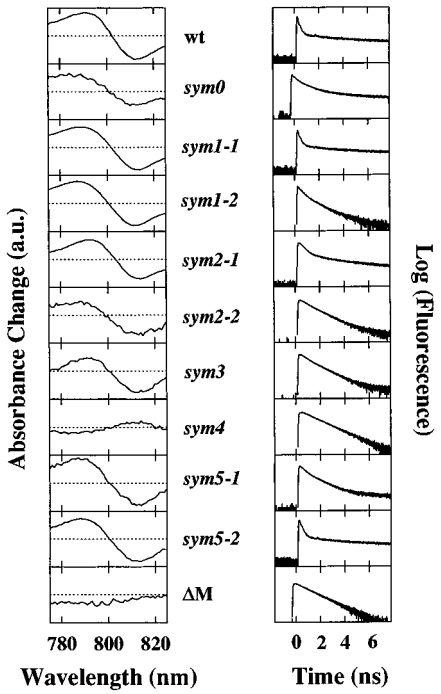

FIGURE 3: Left side: steady state absorbance change observed upon actinic illumination as described in the Experimental Procedures for chromatophores from each of the strains listed. The size of the absorbance changes presented is arbitrarily normalized. The approximate scale factors for each difference spectrum relative to wild type are as follows: wild type, 1; *sym0*, 3; *sym1−1*, 1; *sym1−2*, 1; *sym2−1*, 2; *sym2−2*, 8; *sym3*, 8; *sym4*, 8; *sym5−1*, 8; *sym5−2*, 3; ΔM, 8. Right side: time course of the fluorescence at 900 nm for chromatophores from each strain (see Experimental Procedures). The antenna absorbance at 880 nm and the incident laser intensity were both held constant for each sample. Note that the fluorescence is shown on a log scale in order to show the fluorescence on all time scales recorded. The peak in each case is about 10^4 counts, and the lowest point on each graph is 1 count. Because of this, the τ_A listed in Table 2 is not easily seen on the graph, since in most mutants, the bulk of the decay occurs on the 100 ps time scale or shorter (1% of the total time scale shown) and a factor of 3 decrease in total counts results in only a few-percent drop in the log of the fluorescence value plotted.

components, one for the initial decay and one for the equilibrium repopulation of antenna excited state from $P^+H_A^-$. In each case, three or more decay components are required (analysis not shown). Possible interpretations of this data include static or dynamic heterogeneity in the free energy between the antenna excited singlet state and $P^+H_A^-$ as described previously (Woodbury & Parson, 1986) and some heterogeneity in the properties of the antenna, as might be inferred from the fact that multiple exponential decay components are required to fit the fluorescence from the M subunit deletion strain.

For comparison of the mutants, decays were analyzed in terms of an overall decay time, defined as the integrated area under the decay curve divided by the total initial amplitude of the fluorescence as determined by multiexponential fitting. This overall decay time of the antenna fluorescence is given as τ_A in Table 2. This τ_A is faster in each of the mutants than it is in the ΔM strain, with the exception of *sym4*. The *sym4* mutant shows a τ_A essentially identical to the ΔM strain. Comparing the photosynthetic growth capability of each mutant to the overall decay time of the antenna excited state, one sees that in each case where photosynthetic growth was observed, antenna excited state decay times of less than 300 ps are observed (Table 2).

The decay time τ_D in Table 2 indicates the presence or absence of a multinanosecond decay component in the fluorescence, which has been interpreted in terms of $P^+H_A^-$ formation in the wild type (Woodbury & Parson, 1986). In all of the mutants in which the antenna overall excited state decay time was less than 700 ps, long-lived fluorescence was detected. In most cases, this component's lifetime ranged between 4 and 8 ns, clearly longer than would be expected for the unconnected antenna based on the results from the ΔM mutant. In the case of *sym1* and *sym1−2* (a submutant of *sym1*), the longest-lived fluorescence component has a time constant of only 1.3 ns, but this has been explained previously in terms of a decreased lifetime of $P^+H_A^-$ due to a large increase in the P/P^+ midpoint potential (Taguchi et al., 1992; Stocker et al., 1992).

The fluorescence decay analysis presented in Table 2 suggests that in all the mutants, with the exception of *sym4*, the reaction center is able to trap excitation from the antenna at least to some extent, resulting in $P^+H_A^-$ formation. Generally, the more photosynthetically viable strains were able to trap excitation on faster time scales and this trapping gave rise to a long-lived fluorescence component due to back electron transfer from $P^+H_A^-$. Further quantitation of this fluorescence decay data is difficult without a knowledge of the number of active reaction centers per antenna in each mutant and the effect of the mutation on the energy transfer rate to the reaction center, the charge separation rate, and the yield of charge separation in the reaction center. Some of these topics will be explored below and in the following paper (Lin et al., 1996).

Ability of sym Mutant Reaction Centers to Undergo Stable Charge Separation in Chromatophores. Formation of the state $P^+Q_A^-$ in reaction centers results in a characteristic shift in the 802 nm bacteriochlorophyll band to higher energy. This gives rise to a first-derivative feature in the difference absorbance spectrum in the 775−825 nm region. In the spectrum of chromatophores from U43-based strains (lacking LHII), this wavelength region has relatively little background absorbance due to antenna and, thus, provides a convenient region to detect absorbance changes due to $P^+Q_A^-$ formation in whole photosynthetic membranes.

Figure 3 shows the steady-state absorbance changes for the nine mutants as well as wild type and ΔM chromatophores upon continuous illumination. In all samples, except for *sym4* and ΔM, there is a clear first-derivative feature centered near 800 nm which is indicative of steady-state $P^+Q_A^-$ formation. The magnitudes of the $P^+Q_A^-$ absorbance changes detected from *sym0*, *sym2−2*, *sym3*, *sym5−1*, and *sym5−2* reaction centers were 3−10-fold lower than wild type, *sym1*, *sym1−1*, *sym1−2*, and *sym2−1*. Beyond this, quantification of these steady-state absorbance measurements is difficult since this depends on the number of reaction centers per antenna, the yield of primary photochemistry, and the rate of $P^+Q_A^-$ recombination in each sample.

Isolation and Characterization of Reaction Centers from sym0, sym1−1, sym1−2, sym2−1, sym5−1, and sym5−2. Reaction centers were isolated from wild type, *sym0*, *sym1−1*, *sym1−2*, *sym2−1*, *sym5−1*, and *sym5−2*. With *sym0*, only small amounts of reaction centers could be isolated from the original mutant. Much better yields were obtained by expressing the original *sym0*-containing plasmid in the *sys0−4* genomic background (described below). This background contains a genomic mutation which appears to

Table 3: Time-Resolved Fluorescence Decay[a]

sample	τ_1 (ps)	A_1	τ_2 (ps)	A_2	τ_3 (ps)	A_3	τ_4 (ps)	A_4
wt	9.4	963	121	18.5	728	17.6	4990	1.22
sym0	21.8	866	186	57.9	800	71.5	4860	5.09
sym2−1	41.6	749	155	226	729	19.4	5304	6.11
sym5−2	10.5	928	184	19.5	794	50.4	3930	2.31

[a] Time-resolved fluorescence emission was measured at 910 nm and fitted to the expression $F(t) = A_1e^{-t/\tau_1} + A_2e^{-t/\tau_2} + A_3e^{-t/\tau_3} + A_4e^{-t/\tau_4}$ where $F(t)$ is the observed fluorescence decay as a function of time. Fluorescence amplitudes have been normalized such that $A_1 + A_2 + A_3 + A_4 = 1000$.

enhance the assembly or stability of *sym0* reaction centers. Thus, the amino acid sequence of the L and M subunits is that of the original *sym0* mutation, but it is not known for certain that the H subunit sequence is unchanged (the H subunit gene is located in the genome). Similarly, *sym5−1* reaction centers were also isolated in a suppressor background, *sys5−2*. In the case of the *sys5−2* genomic background, it is likely that the suppressor phenotype is due to reversion in an LHII-coding gene and probably not due to an additional mutation in the H-coding gene (described below). Reaction centers from *sym2−2*, *sym3*, and *sym4* could not be isolated in large enough quantities or sufficient purity to allow characterization.

In each case except *sym5−1*, the ground state absorbance spectra of the isolated reaction centers differed little from the wild type at room temperature except for small (less than 10 nm) shifts in the Q_Y band of P (data not shown), though at low ionic strength, larger shifts of the P band were seen in *sym2−1* (to be described elsewhere). The *sym5−1* mutant showed a roughly 15 nm blue shift of the P band but was otherwise similar to wild type. No further characterization was performed on the *sym5−1*, *sym1−1*, or *sym1−2* reaction centers. Ground state and transient absorbance spectroscopy of *sym0*, *sym2−1*, and *sym5−2* at low temperature will be explored in the following paper in this issue (Lin et al., 1996). The low temperature spectrum of *sym1* (which contains the *sym1−1* and *sym1−2* mutations) was reported previously (Stocker et al., 1992).

Table 3 reports the results of time-correlated single-photon counting measurements for *sym0*, *sym2−1*, and *sym5−2* reaction centers. The fluorescence decay from *sym1* reaction centers was reported previously (Taguchi et al., 1992) and was not repeated for the *sym1* submutants, *sym1−1* and *sym1−2*. For the data shown, excitation was at 860 nm and detection was at 910 nm. Data were recorded over a range of detection wavelengths, and the spectrum of each of the fluorescence decay components reported was similar, peaking near 900−910 nm (uncorrected for the photomultiplier sensitivity), except for the 800 ps component which appears to have a significant contribution in some of the mutants from a pigment which fluoresces at higher energy. All of the samples studied required four exponential decay components for an adequate fit.

Wild type reaction centers show a fast fluorescence decay component whose real lifetime is not resolved completely by our apparatus (the time resolution of our system is about 10 ps in this wavelength region). This component has been assigned to the initial electron transfer event and is itself thought to be composed of two decay components of about 2 and 10 ps (Müller et al., 1992; Hamm et al., 1993; Du et al., 1992). The 100−200 ps component has been assigned to either reaction center heterogeneity or to relaxation of charge-separated states which are able to undergo charge recombination forming P* from $P^+H_A^-$ (Müller et al., 1992; Ogrodnik et al., 1994; Peloquin et al., 1994). The 700−800 ps component is probably a combination of some nonreaction center pigment fluorescence and fluorescence due to charge recombination from $P^+H_A^-$, and the roughly 5 ns component is mostly due to charge recombination from $P^+H_A^-$ (Woodbury & Parson, 1984; Horber et al., 1986; Peloquin et al., 1994).

The fluorescence decay from *sym5−2* is similar to wild type except that the level of the 700−800 ps component is higher, probably due to increased contamination of this mutant preparation by antenna pigment. Both *sym0* and *sym2−1* show significantly longer initial fluorescence decay times than wild type, indicating that primary charge separation may have been affected in these mutants [see the following article in this issue by Lin et al. (1996)]. They also both show a substantially elevated amplitude of their 5 ns fluorescence decay component, indicating a decrease in the standard free energy difference between P* and $P^+H_A^-$ on the nanosecond time scale compared to wild type. Using the initial amplitudes of the long-lived fluorescence components, a 40−60 meV decrease in the standard free energy gap between P* and $P^+H_A^-$ is estimated for *sym2−1* and a 30−40 meV decrease in the same free energy gap for *sym0*. The exact value of the standard free energy gap depends on which fluorescence components are used in the calculation. (The calculation of free energies from fluorescence decay profiles of reaction centers has been discussed previously: Schenck et al., 1982; Woodbury & Parson, 1984; Taguchi et al., 1992; Williams et al., 1992; Ogrodnik et al., 1994; Peloquin et al., 1994). With *sym1* reaction centers, there was a large (roughly 45 meV) decrease in the standard free energy gap between P* and $P^+H_A^-$ as determined from the fluorescence decay measurements (Taguchi et al., 1992). This was due to the introduction of a hydrogen bond between the protein and the ring I acetyl group of P. The new hydrogen bond to P increased the P/P^+ midpoint potential by more than 100 mV (Stocker et al., 1992; Williams et al., 1992; Murchison et al., 1993; Lin et al., 1994).

This leads to the question of whether the P/P^+ midpoint potentials were altered in reaction centers from symmetry mutants other than *sym1*. Table 4 reports the P/P^+ midpoint potential in reaction centers isolated from wild type, *sym0*, *sym2−1*, and *sym5−2*. These measurements were performed by monitoring the bleaching of the Q_Y transition of P at 850 nm while changing the ambient redox potential by either chemically titrating with ferricyanide [see Murchison et al. (1993) for details] or by using an electrochemical cell [see Nagarajan et al. (1993) for details]. The electrochemical titrations were performed in collaboration with Drs. V. Nagarajan and W. Parson at the University of Washington. The *sym0* and *sym5−2* mutants showed midpoint potential changes relative to wild type of less than or equal to 10 mV.

Table 4: P/P^+ Midpoint Potentials

sample	method	E_m (mV)	n[a]
wt	chemical titration	485	1
sym0	chemical titration	490	1
wt	electrochemical	510	1.066
sym2−1	electrochemical	555	1.006
sym5−2	electrochemical	500	1.071

[a] *n* is the factor in the Nernst equation which denotes the number of electrons involved in the reduction/oxidation reaction. For the analysis of the chemical titrations, *n* was assumed to be 1 because the range of the titration only extended to about 80% of the total absorbance change signal that would be observed if complete oxidation of P was obtained. This is because at higher ambient potentials degradation of *sym0* reaction centers occurs. For the electrochemical titrations, complete data was available making it possible to accurately determine *n*. The statistical error in all of the chemical and electrochemical data is about ±10 mV.

Table 5: General Characteristics of the Suppressor/Revertant Strains

parent	sup/rev[a]	genome[b]	plasmid[b]	mutation[c]
sym0	*sys0−1*	5	0	unknown
sym0	*sym0R−4*	0	1	FV(M173)
sym2−2	*sym2R−4a*	0	6	AV(M213)
sym2−2	*sym2R−10*	0	1	LM(M220)
sym2−2	*sym2R−13*	0	1	LQ(M220)
sym2−2	*sym2R−14*	0	1	LV(M220)
sym5−1	*sys5−1*	4	0	$LHII^+$

[a] Mutated gene in each suppressor strain is indicated with a representative allele number following the hyphen. Genomic suppressor mutations are referred to as *sys* mutants. Suppressors located on the plasmid are referred to by the original plasmid name with an "R" appended. [b] Number of isolates. [c] Mutational event in suppressor strain.

The *sym2−1* mutant showed a nearly 50 mV P/P^+ midpoint potential increase relative to wild type (Table 4).

Time-resolved spectroscopy of the early electron transfer reactions in *sym0*, *sym2−1*, and *sym5−2* reaction centers will be described in the following article in this issue (Lin et al., 1996).

Suppressor Analyses of sym Mutants. Suppressor mutations were isolated from *sym2−2* under high illumination (12 in. away from twelve 60 W Lumiline bulbs). Colonies from 22 independent phenotypic revertants were purified by a second photosynthetic growth in stab cultures followed by streaking on plates incubated aerobically in the dark. The resulting single colonies were retested for photosynthetic ability in stabs, verifying that each strain was capable of vigorous photosynthetic growth. These suppressor mutations will be referred to as *sym2R* mutations.

To determine if the *puf* operon containing plasmid from each *sym2R* suppressor strain was sufficient for the suppressor phenotype, plasmid was isolated from each *sym2R* strain and remated into the Puf^- *Rb. capsulatus* host strain, U43. Plasmid from all but one of the 22 suppressor strains was able to confer the ability to grow photosynthetically in stab cultures on U43, indicating that one or more suppressor mutations were present on at least 21 of the *sym2R* plasmids. Nine *sym2R* plasmids were sequenced through the 160 base *Xmn*I−*Sac*II region surrounding the *sym2−2* mutation. In addition to the original *sym2−2* mutation, the single amino acid changes noted in Table 5 were identified.

Reaction centers were isolated from two of the *sym2−2* suppressor strains. Since both the original *sym2−2* mutation and its suppressors involved amino acid changes near Q_A, transient absorbance change signals due to $P^+Q_A^-$ formation and recombination were measured. The sample was excited with a roughly 5 ns duration pulse from a doubled Nd:YAG laser and probed with a continuous 860 nm measurement beam from an argon ion laser-pumped titanium sapphire laser. Surprisingly, the size of the initial absorbance change signal from the two *sym2−2* suppressors was roughly 20-fold smaller than that from wild type reaction centers using the same reaction center concentration and excitation light intensity (data not shown). In contrast, the initial $P^+Q_A^-$ signal from chromatophores of the *sym2−2* suppressors was only about a factor of 2 lower than that observed for wild type (data not shown). Apparently, the ability to undergo electron transfer in the *sym2−2* suppressor strains is largely intact in the chromatophores but is almost completely lost upon reaction center isolation.

All of the photosynthetically enhanced suppressors isolated upon photosynthetic selection using *sym5−1* in U43 showed the spectral characteristics of the LHII antenna (800 and 850 nm absorbance peaks in the chromatophore preparations), indicating that the suppressor phenotype was due to a reversion of the mutation in the LHII-coding gene. Expression of *sym5−1* in an $LHII^+$ strain, ΔRC6, also resulted in photosynthetic growth, confirming that reversion of the LHII point mutation in the original U43 deletion strain could result in enhancement of photosynthetic growth in *sym5−1*. Expressing the mutants that were unable grow photosynthetically in the U43 deletion background (*sym0, sym2−2, sym3,* and *sym4*) in the $LHII^+$ ΔRC6 background did not result in phenotypic reversion to photosynthetic growth.

Five independent suppressor strains were isolated from the parental *sym0* strain using a slightly less intense light source than was used for *sym2−2* (9−15 in. away from two 60 W Lumiline bulbs). Curing and remating experiments addressed the possibility of the genomic origin of the *sym0R* suppressor phenotype. Plasmid was isolated from each *sym0R* strain and remated into the non-suppressor, *puf* operon deletion strain, U43. Also, each *sym0R* strain was cured (Magnin et al., 1987) of *sym0R* plasmid and either *sym0* or *sym0R* plasmid was mated back in. Photosynthetic ability was compared by growth in stabs for each of the newly constructed strains, and for the original *sym0* (U43 with *sym0* plasmid) and *sym0R* isolates. Photosynthetic ability required the presence of the *sym0R* genomic backgrounds in four of the five strains. For one *sym0R* strain (*sym0R−4*) the suppressor phenotype was obtained when either the *sym0R−4* plasmid was introduced into fresh U43 cells or the cured *sym0R−4* cells (referred to as *sys0−4*) were complemented with a fresh *sym0* plasmid, indicating the presence of at least two suppressor mutations, one in the genome and one on the *puf* plasmid either of which results in the suppressor phenotype. Sequencing of the 0.9 kb *Kpn*I−*Bam*HI fragment from a *sym0R−4* plasmid demonstrated the presence of a new FV(M173) mutation within the original *sym0* mutation.

A prominent absorbance peak centered at about 850 nm has been observed in almost all second site suppressor strains of *Rb. capsulatus*−*Chloroflexus aurantiacus* chimeric reaction center mutants when antenna and reaction center genes are nonfunctional (Gallo, 1994). Sonicates from five *sym0* genomic suppressor strains which had been cured of their original *sym0* plasmids containing the LHI and reaction center genes were examined for the presence of this absorbance peak. Only one of the strains yielded this

absorbance peak in the difference spectra resulting from subtraction of the parental U43 background strain absorbance (data not shown).

DISCUSSION

Overall Asymmetry Requirements for Photosynthetic Activity. Perhaps the most striking result from this study is that local asymmetry in the amino acid sequences which define the environment of the cofactors involved in initial electron transfer and their B side counterparts (P, B_A, B_B, H_A, and H_B) is generally not a requirement for overall photosynthetic function. Local asymmetry is used here to mean asymmetry between the L and M subunits at one or a small number of consecutive residues. The large-scale mutants *sym0*, *sym1−1*, *sym1−2*, *sym2−1*, *sym5−1*, and *sym5−2* between them convert about 80% of the M subunit amino acids which are closely associated with P, B_A, B_B, H_A, and H_B to the corresponding L subunit amino acids. This means that between these mutants, 80% of the environment of these cofactors is made symmetric, though only a small number of amino acids are involved in each particular mutation. With the exception of *sym0*, all of these mutants are able to grow photosynthetically and in the case of *sym0*, only one amino acid change is required to restore photosynthetic growth (Table 5).

A couple of important points about the conclusions outlined above require emphasis. First, this does not mean that either the M or the L subunit sequence can be used at any of the amino acid sites in question. Only the M subunit amino acids were changed in this study; the L subunit amino acids were left intact. However, by looking at the cofactors closely associated with particular amino acids in Figure 2 [compiled from the structural information of Allen et al. (1988), Yeates et al. (1988), and El-Kabbani et al. (1991)], one can quickly see that the relatively small effects of introducing local symmetry cannot be explained simply by saying that all of the amino acids important for defining the environment of the A side cofactors are on the L subunit of the reaction center. Obviously, half of the environment of P is defined by the M subunit (Figure 2). More than half of the amino acids close to B_A which differ from their counterparts close to B_B are also part of the M subunit (including the important interaction at tyrosine M208; Nagarajan et al., 1990, 1993; Hamm et al., 1993; Finkele et al., 1990; Gray et al., 1990; Figure 2), and similarly the environment of H_A is defined both by M and L amino acids (Figure 2). Thus, M subunit amino acids probably play as important a role in defining the asymmetric characteristics of the early A side electron transfer reactions as do the L subunit amino acids.

The second point to bear in mind is that only amino acids which are different between the L and M subunits are being considered in this study. Obviously, an amino acid which is identical on both sides, even though it may be of critical importance for electron transfer will not affect the results. This study shows that asymmetry *per se* is not essential in the region of the cofactors involved in initial electron transfer at the amino acid positions that were changed. It does not necessarily say what amino acid properties *are* essential at these positions.

Local asymmetry has a greater effect on overall photosynthetic function in the amino acid sequences that make up the cytoplasmic end of the reaction center. One might expect this given the very different known roles of Q_A and Q_B (Okamura & Feher, 1995). Most of the close asymmetric interactions between the protein and either Q_A or the nonheme iron are defined by *sym2−2* and *sym4* (Figure 2). Neither of these mutants is capable of photosynthetic growth.

However, it is probably not primarily the loss of activity in structurally intact reaction centers that causes the loss of photosynthetic growth capability in *sym2−2* and *sym4*. For both of these mutants, and for *sym3*, SDS−PAGE electrophoresis of chromatophore proteins showed little to no evidence for the presence of the reaction center protein subunits. Additional evidence for assembly/stability problems in these mutants comes from the fact that the chlorophyll absorbance per mg protein in photosynthetic membranes was also very low (Table 2). The latter observation is consistent with observations of reaction center deletion mutants, such as ΔM, which lack not only the reaction center but a large fraction of the LHI antenna bacteriochlorophyll as well (Table 2). Apparently, the stability of the two complexes is linked in the U43 strain.

Thus, the primary deficiency in these mutants is apparently overall reaction center assembly or stability, rather than the ability of assembled reaction centers to function. With *sym2−2* and *sym3*, there was evidence for a small amount of charge separation in chromatophores as well as a fluorescence decay signature for the formation of $P^+H_A^-$ (Table 2, Figure 3). This suggests that the small number of reaction centers that were present in the membrane were capable of charge separation.

Detailed Analysis of the sym0 Region. The *sym0* mutation is shown in Figures 1 and 2. There are nine amino acid changes involved. Of these, M184(T→V) comes in close contact with P and B_B, M185(N→S) comes in close contact with P, and M173(P→F) comes in close contact with B_B and the carotenoid (C). For the purposes of this report, close contact amino acids are those identified in the reaction center structural literature (Allen et al., 1988; Yeates et al., 1988; El-Kabbani et al., 1991) as being within 4 Å of a reaction center cofactor. There are, of course, other amino acids than the three identified above in the *sym0* region which come in close contact with reaction center cofactors. However, these are the only three that come in close contact and are different between the L and M subunits.

Of the 22 asymmetric amino acids changed near the cofactors involved in the initial electron transfer reaction, only at M173 (the corresponding L amino acid is L146) in *sym0* must local asymmetry be maintained for viable photosynthetic growth to occur. M173 is a proline in wild type *Rb. capsulatus*. It was changed to a phenylalanine in *sym0* and in this mutant, photosynthetic growth was not observed (Table 2). As shown in Table 5, it was possible to isolate two classes of suppressors to *sym0*. The first class of suppressors simply converted M173 from a phenylalanine to a valine. Since valine is found at this position in wild type *Rb. sphaeroides*, *Rhodospirillum rubrum*, and *Rp. viridis* (Komiya et al., 1988), this can be viewed as a change back to a wild type or at least a naturally occurring amino acid at this position. Even this change, however, is not an absolute requirement for reaction center function since a second site suppressor somewhere in the genome also results in the ability to grow photoheterotrophically (Table 5).

In fact, the inability of *sym0* to grow photosynthetically is probably due primarily to problems with assembly or stability of the *sym0* reaction center complex, much as was the case for *sym2−2*, *sym3*, and *sym4*. Evidence for assembly/stability problems in *sym0* comes from the fact that SDS−PAGE showed that the level of reaction center protein was dramatically decreased and the chlorophyll absorbance per mg of protein in photosynthetic membranes was also very low (Table 2) as discussed above for other mutants which could not grow photosynthetically.

M173 apparently plays an important role in the structural integrity of the reaction center. The proline normally found in the *Rb. capsulatus* M subunit at this position is part of a tight turn (extrapolating from the *Rb. sphaeroides* structure). Most likely the phenylalanine present at this position on the L side changes the local structure in the turn region. It is possible that M173 is important in defining the interface between the carotenoid binding pocket and the B_B binding site since M173 comes in close contact with both cofactors. Thus, insertion of a large amino acid like phenylalanine at this position may destabilize binding of both cofactors.

The M184(T→V) and M185(N→S) changes in the *sym0* region, which are close to P, apparently have little effect on its midpoint potential (Table 4). They probably do affect the spectral properties of P and B_B [see Lin et al. (1996), which follows this report]. The 30−40 meV increase in the apparent free energy of $P^+H_A^-$ relative to P*, as estimated from the fluorescence decay measurements, cannot be explained by the observed 5 mV change in the P/P^+ midpoint potential and suggests effects on the H_A/H_A^- midpoint potential or the formation of an additional long-lived fluorescence state.

Detailed Analysis of the sym1 Region. The *sym1* mutation has been discussed previously. The large increase in P/P^+ midpoint potential as well as some of the electrosorption and EPR spectral properties that differ in the *sym1* mutation from the wild type appear to be due to the M195 mutation of phenylalanine to histidine (Stocker et al., 1992; Taguchi et al., 1992). It is now clear that a histidine at position M195 results in the introduction of a new hydrogen bond to a ring I acetyl group of P (Mattioli et al., 1994, 1995) and that such hydrogen bonding interactions result in substantial increases in the P/P^+ redox potential [Stocker et al., 1992; Williams et al., 1992; Lin et al., 1994; Murchison et al., 1993; see Allen and Williams (1995) for a review]. Though *sym1* itself has significantly impaired photosynthetic growth characteristics, *sym1−1* and *sym1−2* both grow at rates almost equivalent to wild type. In addition, the overall rate of antenna excitation quenching in these mutants is only slightly longer than wild type (70 vs 40 ps, Table 2) and both show stable $P^+Q_A^-$ formation under actinic illumination (Table 2, Figure 3). An obvious difference between the two mutations is that the apparent lifetime of $P^+H_A^-$, as estimated from the fluorescence measurements in chromatophores, is much shorter in *sym1−2* (1.3 ns) compared to either wild type or *sym1−1* (roughly 8 ns). This is presumably due to a higher P/P^+ midpoint potential in *sym1−2* which increases the driving force for recombination in the state $P^+H_A^-$. The fact that *sym1−1* shows an essentially wild type $P^+H_A^-$ lifetime suggests that there is little perturbation of the P/P^+ midpoint potential in this mutant; however, direct measurements have not been made. The *sym1−1* mutation is essentially identical to wild type in all respects measured suggesting that neither the M187(F→T) nor the M188(S→G) mutations, which both involve positions in close contact with P, have major phenotypic effects, though detailed spectroscopy on this mutant has not been performed. Interestingly, there are also two other mutations in *sym1−1* which do not come in close contact with any cofactors but may represent large changes in amino acid polarity. Two potentially charged groups, Asp(M190) and His(M191) are changed to less polar amino acids (Thr and Tyr, respectively). These also apparently have little effect on overall reaction center function.

Since the phenotype of *sym1−2* is dominated by the M195(F→H) mutation and the resulting change in the P/P^+ midpoint potential, it would be difficult to detect smaller effects of the other amino acids which were changed in this region. However, none of the changes present in *sym1−2* has a significant effect on photosynthetic growth rates as assayed in this report. This conclusion applies to the above mentioned M195(F→H) mutation, as well as the M194(L→F) and M203(S→G) mutations, which are in close contact with P, and the M201(G→M) mutation, which is in close contact with B_A.

Detailed Analysis of the sym2 Region. The *sym2* region extends down most of the D helix of the M subunit of the reaction center (Figures 1 and 2). This region strongly overlaps with a previous symmetry mutation in *Rb. capsulatus*, the so-called D_{LL} mutant of Robles et al. (1990) which covers Gly(M192) through His(M217). Revertant/suppressor analysis of the D_{LL} mutant influenced the design of *sym2−1* and *sym2−2*. From that analysis it was predicted that Leu(M212) was critical for binding of H_A, since the original D_{LL} mutant lacked H_A and this cofactor was restored by a single reversion event at M212. For this reason, Leu(M212) was not changed as part of either *sym2−1* or *sym2−2*.

The *sym2−1* mutation contains three asymmetric amino acid sites that are in close contact with reaction center cofactors in the *Rb. sphaeroides* structure: M205(A→S) near B_A, M207(L→F) near P, and M208(Y→F) near P, B_A, and H_A (Figure 2). This mutant grows well photosynthetically (Table 2) but results in substantially slower energy trapping from the antenna (Table 2) and an increased P/P^+ midpoint potential (Table 4). Past studies of the M208(Y→F) mutation (Nagarajan et al., 1990, 1993; Finkele et al., 1990; Jia et al., 1993) have shown that this change both slows down the initial electron transfer rate (from 3.5 to about 10 ps) and increases the P/P^+ midpoint potential (from about 500 mV to about 530 mV). The midpoint potential change roughly corresponds to that observed here (the exact value of the midpoint potential of *sym2−1* depends on ionic strength, pH, and detergent conditions, a topic that will be discussed in a future publication). The change in the reaction center charge separation rate seen at room temperature for the M208(Y→F) mutation, however, is probably not large enough to explain the decrease in the rate of energy trapping in the antenna. The excitation quenching in the LHI antenna is rate limited primarily by the speed of energy transfer between the antenna and the reaction center, not by the rate of charge separation itself [Xiao et al., 1994; see also Visscher et al. (1989), Timpmann et al. (1993), Otte et al. (1993), and Beekman et al. (1994) for similar work in other purple bacteria], and less than a 2-fold change in excitation trapping rate is expected upon slowing electron transfer from 3.5 to 10 ps [estimated from the kinetic model presented in Xiao et al. (1994)]. As

will be shown in the following paper (Lin et al., 1996), the electron transfer rate is much slower in *sym2−1* than it is in the single M208(Y→F) mutation.

The *sym2−2* mutation includes three asymmetric amino acids which are in close contact with Q_A: M213(L→A), M220(T→L), and M221(I→V). Note that M213(L→A) is included in the D_{LL} mutant (Robles et al., 1990), and revertant/suppressor analysis suggested that asymmetry at this site was not required for restoration of photosynthetic growth. Like the D_{LL} mutant, *sym2−2* is unable to grow under photoheterotrophic conditions, but suppressors can be isolated. Suppressor analysis of *sym2−2*, however, shows that restoration of asymmetry at M213 is one method of recovering photosynthetic growth in this mutant. The majority of suppressors isolated involved an Ala to Val change at this position (Table 5). The remaining suppressors isolated changed Leu(M220) in *sym2−2* to either Met, Gln, or Val (Table 5). The amino acid usage at M213 and M220 is identical in four species of photosynthetic bacteria, as is the amino acid usage at the corresponding positions in the L subunit (Komiya et al., 1988). The apparent inconsistency between these studies and those of Robles et al. (1990) concerning the role of M213 can be resolved by recognizing that the D_{LL} mutant did not change M220 and suppression of *sym2−2* can be achieved either by secondary mutations at M213 or M220.

As described in the Results, the $P^+Q_A^-$ signal formed upon excitation of chromatophores of the *sym2−2* suppressor mutations was smaller, but of the same order of magnitude as the chromatophore signal from wild type under the same sample and illumination conditions. However, the signal from isolated reaction centers of the *sym2−2* suppressors was 20-fold lower than the comparable wild type signal. Thus, it is likely that Q_A is lost upon reaction center isolation in *sym2−2* implying a much more loosely bound quinone in this reaction center than in the wild type. This may make sense in terms of the relatively stronger binding of Q_A vs Q_B in wild type reaction centers, remembering that the *sym2−2* mutation effectively replaces part of the Q_A pocket with that of Q_B. The tendency of Q_A to be only weakly bound may be much more pronounced in the original *sym2−2* mutant than in its suppressors since quinone interactions at both M213 and M220 are changed in the original mutant. A more loosely bound Q_A in *sym2−2* suggests a more open reaction center structure, and this in turn could lead to a less stable reaction center.

Both M213 and M220 are within 4 Å of Q_A, and M220 is apparently hydrogen bonded to one of the quinone carbonyl groups (El-Kabbani et al., 1991; Allen et al., 1988). A previous study of a Thr to Val change at the M222 position in *Rb. sphaeroides* (which is analogous to the M220 position of *Rb. capsulatus*) also concluded that this threonine is important for quinone binding (Stilz et al., 1994).

Detailed Analysis of the sym3 Region. One of the least homologous regions between the L and M subunits is the loop region included in the *sym3* mutation (Figures 1 and 2). None of the 13 amino acids that were changed in the M subunit was identical to their L subunit counterparts, and at seven of the 13 positions there are no corresponding L amino acids [in this region of the alignment between the L and M subunits, a seven amino acid gap exists in the L sequence; see Figure 2 and Michel et al. (1986)]. The *sym3* mutant cannot grow photoheterotrophically (Table 2) and there is little reaction center protein visible on Coomassie-stained SDS−PAGE implying that reaction centers are either not assembled or not stable. Only weak $P^+Q_A^-$ signals can be seen in light-minus-dark difference spectra, and there is only a small amount of long-lived fluorescence indicative of $P^+H_A^-$ formation (Table 2, Figure 3). This region includes only one amino acid which comes in close contact with a reaction center cofactor in the *Rb. sphaeroides* structure, and that is Glu(M234), the bidentate ligand to the nonheme iron atom. Exactly what one considers this Glu to have been replaced by in the *sym3* mutation is difficult to say. In the alignment of Michel et al. (1986) it appears aligned with a Gly on the L subunit, but the gap placement in this region is not well defined. However, previous single site mutagenesis of this Glu has indicated that its liganding properties are not essential for photosynthetic growth (Wang et al., 1992). Evidently, the large structural perturbation caused by removing the seven amino acids normally present in the M subunit that are absent in the L subunit results in instability. One probable reason for this is that the M subunit amino acid sequence in this region contains a series of charged residues between M230 and M234 which are thought to be involved in numerous salt bridge interactions with other charged groups on the L, M, and H subunits (Chang et al., 1991). Removal of these charged groups disrupts the ionic interactions and potentially destabilizes both the local structure of the M subunit and the subunit−subunit interactions.

Detailed Analysis of the sym4 Region. More than half of the asymmetric amino acids closely associated with Q_A are included in the *sym4* mutation (Figure 2). Like *sym3*, this region of the amino acid sequence is very poorly conserved between L and M. The *sym4* mutant is the one mutant in this series that showed absolutely no charge separation capability in photosynthetic membranes (Table 2, Figure 3). Judging by the lack of reaction center protein visible on SDS−PAGE, this mutant either does not assemble reaction centers or is very unstable. Unfortunately, it was not possible to isolate suppressors to this mutation. This coupled with the complete lack of photosynthetic function makes it difficult to say very much about the role of asymmetry at specific amino acid positions in this region. However, many of the amino acid replacements from the L subunit in this region represent large changes in amino acid polarity. For example, M246 and M247 are both alanine, but the corresponding amino acids in the L subunit are Glu(L212) and Asp(L213), which are thought to be involved in proton uptake during electron transfer to Q_B (Okamura & Feher, 1995), and are potentially charged. As was the case for *sym3*, there may be stabilizing interactions in the wild type Q_B pocket between these potentially charged groups and other groups in the protein. The same level of charge stabilization may not be present when this section is transferred into the M subunit. In addition, Trp(M252) is thought to be important for Q_A binding (Stilz et al., 1994) and may play a role in stability, much as was discussed for *sym2−2*.

Detailed Analysis of the sym5 Region. The *sym5* region contains most of the E helix (Figure 2). Most of this region is included in the *sym5−1* submutant which contains the amino acids that interact strongly with Fe, Q_A, and H_B (Figure 2). The *sym5−2* mutant alters the upper part of the E helix which interacts with P (Figure 2). The *sym5−1* mutant

grows only very weakly under photoheterotrophic conditions. As was the case for *sym0*, *sym2−2*, *sym3*, and *sym4*, the SDS−PAGE results and the chlorophyll absorbance per gram of protein (Table 2) indicate either that reaction centers do not assemble properly in this mutant or that they are not stable. The few reaction centers that are present appear to undergo stable charge separation (Figure 3). Suppressor analysis of this mutant did not result in any suppressor mutations within the *puf* operon. Instead, photosynthetic activity could be restored by reversion of the LHII point mutation in the U43 background strain (see above). This implies that the *sym5−1* reaction centers are basically functional, but apparently inefficient.

The *sym5−1* mutation contains four asymmetric amino acids in close contact with reaction center cofactors: M266-(W→L) near Q_A and M272(V→L), M274(V→A), and M275-(T→V) near H_B. It is not obvious which, if any, of these changes destabilize the reaction center structure. Additional changes that are more distant from the cofactors may have serious structural consequences such as M261(E→L) which results in the loss of a potentially charged group (Figure 2).

The *sym5−2* mutation involves one asymmetric amino acid which is in close contact with P: Gly(M278) is changed to a Ser. There are essentially no obvious differences between *sym5−2* and wild type in terms of the ability to quench antenna fluorescence or undergo charge separation forming the state $P^+Q_A^-$. As will be shown in the following article, the initial photochemistry of this mutant is also essentially that of wild type (Lin et al., 1996). Under photosynthetic growth conditions, it does grow somewhat more slowly than wild type, but there is no obvious problem with the isolated reaction centers, implying that the five amino acid changes in this mutation do not have a major effect on the electron transfer properties of the reaction center.

Possible Identities of Genomic Suppressors. Several of the suppressor strains isolated involved mutations in the bacterial genome rather than plasmid-borne mutations. In most cases, there is little data indicating what genes may be involved in these mutations. However, for two of the suppressors, possible genomic functions can be suggested. In the case of *sym5−1*, it is very likely that the genomic suppressor is really a reversion of the $LHII^-$ point mutation in U43. The evidence for this comes from the spectroscopic data showing the presence of LHII complexes in the membrane and the fact that the ability of *sym5−1* to grow photosynthetically is greatly enhanced by expression of the *sym5−1* plasmid in a background strain containing a functional LHII gene.

One of the *sym0* suppressor mutations, *sys0−5*, results in the production of a complex that absorbs at 850 nm. A similar absorbance peak at 855 nm has been observed previously and has been attributed to a pigment (pheophorbide) aggregate or complex called P855 (Richards & Fidai, 1990; Young & Marrs, 1990). The P855 absorbance band was present only when the *pufQ* gene was added in *trans* in *Rb. capsulatus* strains lacking the *puc* (LHII-coding) and *puf* (LHI, PufL, PufM-coding) operons but not when the *pufQ* gene was absent. The PufQ protein itself is unlikely to be a component of P855 since P855 accumulation as well as tetrapyrrole precursor accumulation can be induced with NMP (*N*-methylprotoporphyrin), a ferrochelatase inhibitor (Richards & Fidai, 1990), in *pufQ* deletion strains (Young & Marrs, 1990). Thus, NMP increases the ratio of porphyrin which is used for bacteriochlorophyll synthesis vs heme synthesis. It is possible that the *sys0−5* mutation, as well as genomic suppressors previously isolated using other large-scale mutations (Gallo, 1994), may also involve mutations which change the relative amounts of bacteriochlorophyll vs heme made by the cell.

Conclusions. Though there were significant and interesting effects of the nine large-scale symmetry mutations studied here on reaction center electron transfer properties and stability, there were surprisingly no cases in which loss of photosynthetic growth capability occurred purely due to the loss of reaction center function. In fact, in all mutants but one it was possible to demonstrate the presence of reaction centers capable of undergoing electron transfer at least to Q_A. This suggests that asymmetry is not an absolute functional requirement in the reaction center, lending support to the concept of an ancestral homodimer reaction center. However, in its present form, the reaction center requires some asymmetry either in the assembly process or for reaction center stability once assembly is complete.

ACKNOWLEDGMENT

We thank S. Bond, C.-K. Chiou, H. Murchison, K. Carty, and M. Li for their help with plasmid constructions, reaction center isolation, and suppressor analysis. The authors also thank S. Cohen for the gift of *Rb. capsulatus* strain ΔRC6, V. Nagarajan and W. Parson for performing the electrochemical midpoint potential measurements and for critical reading of the manuscript, and J. Allen and J. Williams for helpful discussions.

REFERENCES

Allen, J. P., & Williams, J. C. (1995) *J. Bioenerg. Biomembr. 27*, 275−283.
Allen, J. P., Feher, G., Yeates, T. O., Komiya, H., & Rees, D. C. (1987) *Proc. Natl. Acad. Sci. U.S.A. 84*, 5730−5734.
Allen, J. P., Feher, G., Yeates, T. O., Komiya, H., & Rees, D. C. (1988) *Proc. Natl. Acad. Sci. U.S.A. 85*, 8487−8491.
Beekman, L. M. P., van Mourik, F., Jones, M. R., Visser, H. M., Hunter, C. N., & van Grondelle, R. (1994) *Biochemistry 33*, 3143−3147.
Chang, C.-H., El-Kabbani, O., Tiede, D., Norris, J., & Schiffer, M. (1991) *Biochemistry 30*, 5352−5360.
Chen, C.-Y., Beatty, J. T., Cohen, S. N., & Belasco, J. G. (1988) *Cell 52*, 609−619.
Coleman, W. J., & Youvan, D. C. (1993) *Nature 366*, 517−518.
Deisenhofer, J., Epp, O., Miki, K., Huber, R., & Michel, H. (1984) *J. Mol. Biol. 180*, 385−398.
Du, M., Rosenthal, S. J., Xie, X., DiMagno, T. J., Schmidt, M., Hanson, D. K., Schiffer, M., Norris, J. R., & Fleming, G. R. (1992) *Proc. Natl. Acad. Sci. U.S.A. 89*, 8517−8521.
El-Kabbani, O., Chang, C.-H., Tiede, D., Norris, J., & Schiffer, M. (1991) *Biochemistry 30*, 5361−5369.
Ermler, U., Fritzsch, G., Buchanan, S. K., & Michel, H. (1994) *Structure 2*, 925−936.
Feher, G., Allen, J. P., Okamura, M. Y., & Rees, D. C. (1989) *Nature 339*, 111−116.
Finkele, U., Lauterwasser, C., Zinth, W., Gray, K. A., & Oesterhelt, D. (1990) *Biochemistry 29*, 8517−8521.
Gallo, D. M, Jr. (1994) Ph.D. Thesis, Arizona State University, Tempe, Arizona.
Gehlen, J. N., Marchi, M., & Chandler, D. (1994) *Science 263*, 499−502.
Gray, K. A., Farchaus, J. W., Wachtveitl, J., Breton, J., & Oesterhelt, D. (1990) *EMBO J. 9*, 2061−2070.
Hamm, P., Gray, K. A., Oesterhelt, D., Feick, R., Scheer, H., & Zinth, W. (1993) *Biochim. Biophys. Acta 1142*, 99−105.

Horber, J. K. H., Gobel, W., Ogrodnik, A., Michel-Beyerle, M. E., & Cogdell, R. J. (1986) *FEBS Lett. 198*, 273−278.
Jia, Y., DiMagno, T. J., Chan, C.-K., Wang, Z., Du, M., Hanson, D. K., Schiffer, M., Norris, J. R, Fleming, G. R., & Popov, M. S. (1993) *J. Phys. Chem. 97*, 13180−13191.
Kirmaier, C., & Holten, D. (1987) *Photosynth. Res. 13*, 225−260.
Kirmaier, C., & Holten, D. (1993) in *The Photosynthetic Reaction Center* (Deisenhofer, J., & Norris, J. R., Eds.) Vol. 2, pp 49−70, Academic Press, San Diego, CA.
Kirmaier, C., Holten, D., & Parson, W. W. (1985) *Biochim. Biophys. Acta 810*, 33−48.
Komiya, H., Yeates, T. O., Rees, D. C., Allen, J. P., & Feher, G. (1988) *Proc. Natl. Acad. Sci. U.S.A. 85*, 9012−9016.
Lin, S., Xiao, W., Eastman, J. E., Taguchi, A. K. W., & Woodbury, N. W. (1996) *Biochemistry 35*, 3187−3196.
Lin, X., Murchison, H. A., Nagarajan, V., Parson, W. W., Allen, J. P., & Williams, J. C. (1994) *Proc. Natl. Acad. Sci. U.S.A. 91*, 10265−10269.
Lockhart, D. J., Kirmaier, C., Holten, D., & Boxer, S. G. (1990) *J. Phys. Chem. 94*, 6987−6995.
Magnin, J.-P., Willison, J. C., & Vignais, P. M. (1987) *FEMS Microbiol. Lett. 41*, 157−161.
Martin, J.-L., & Vos, M. H. (1992) *Annu. Rev. Biophys. Biomol. Struct. 21*, 199−222.
Mattioli, T. A., Williams, J. C., Allen, J. P., & Robert, B. (1994) *Biochemistry 33*, 1636−1643.
Mattioli, T. A., Lin, X., Allen, J. P., & Williams, J. C. (1995) *Biochemistry 34*, 6142−6152.
Michel, H., & Deisenhofer, J. (1988) *Biochemistry 27*, 1−7.
Michel, H., Weyer, K. A., Gruenberg, H., Dunger, I., Oesterhelt, D., & Lottspeich, F. (1986) *EMBO J. 5*, 1149−1158.
Müller, M. G., Griebenow, K., & Holtzwarth, A. R. (1992) *Chem. Phys. Lett. 199*, 465−469.
Murchison, H. A., Alden, R. G., Allen, J. P., Peloquin, J. M., Taguchi, A. K. W., Woodbury, N. W., & Williams, J. C. (1993) *Biochemistry 32*, 3498−3505.
Nagarajan, V., Parson, W. W., Gaul, D., & Schenck, C. C. (1990) *Proc. Natl. Acad. Sci. U.S.A. 87*, 7888−7892.
Nagarajan, V., Parson, W. W., Davis, D., & Schenck, C. C. (1993) *Biochemistry 32*, 12324−12336.
Ogrodnik, A., Keupp, W., Volk, M., Aumeier, G., & Michel-Beyerle, M. E. (1994) *J. Phys.Chem. 98*, 3432−3439.
Okamura, M. Y., & Feher, G. (1995) in *Anoxygenic Photosynthetic Bacteria* (Blankenship, R. E., Madigan, M. T., & Bauer, C. E., Eds.) pp 577−594, Kluwer Academic Publishers, Dordrecht, The Netherlands.
Otte, S. C. M., Kleinherenbrink, F. A. M., & Amesz, J. (1993) *Biochim. Biophys. Acta 1143*, 84−90.
Parson, W. W. (1991) in *Chlorophylls* (Scheer, H., Ed.) pp 1153−1180, CRC Press, Boca Raton, FL.
Parson, W. W., Chu, Z.-T., & Warshel, A. (1990) *Biochim. Biophys. Acta 1017*, 251−272.
Peloquin, J. M., Williams, J. C., Lin, X., Alden, R. G., Taguchi, A. K. W. , Allen, J. P., & Woodbury, N. W. (1994) *Biochemistry 33*, 8089−8100.
Peterson, G. L. (1977) *Anal. Biochem. 83*, 346−356.
Prince, R., & Youvan, D. C. (1987) *Biochim. Biophys. Acta 890*, 286−291.
Richards, W. R., & Fidai, S. (1990) in *Molecular Biology of Membrane-Bound Complexes in Phototrophic Bacteria* (Drews, G., & Dawes, E. A., Eds.) pp 253−260, Plenum Press, New York.
Robles, S. J., Breton, J., & Youvan, D. C. (1990) *Science 248*, 1402−1405.
Schenck, C. C., Blankenship, R. E., & Parson, W. W. (1982) *Biochim. Biophys. Acta 680*, 44−59.
Steffen, M. A., Lao, K., & Boxer, S. G. (1994) *Science 264*, 810−816.
Stilz, H. U., Finkele, U., Holzapfel, W., Lauterwasser, C., Zinth, W., & Oesterhelt, D. (1994) *Eur. J. Biochem. 223*, 233−242.
Stocker, J. W., Taguchi, A. K. W., Murchison, H. A., Woodbury, N. W., & Boxer, S. G. (1992) *Biochemistry 31*, 10356−10362.
Taguchi, A. K. W., Stocker, J. W., Alden, R. G., Causgrove, T. P., Peloquin, J. M., Boxer, S. G., & Woodbury, N. W. (1992) *Biochemistry 31*, 10345−10355.
Taguchi, A. K. W., Stocker, J. W., Boxer, S. G., & Woodbury, N. W. (1993) *Photosynth. Res. 36*, 43−58.
Timpmann, K., Zhang, F. G., Freiberg, A., & Sundstrîm, V. (1993) *Biochim. Biophys. Acta 1183*, 185−193.
Wang, X., Cao, J., Maroti, P., Stilz, H. U., Finkele, U., Lauterwasser, C., Zinth, W., Oesterhelt, D., Govindjee, & Wraight, C. A. (1992) *Biochim. Biophys. Acta 1100*, 1−8.
Williams, J. C., Steiner, L. A., Feher, G., & Simon, M. I. (1984) *Proc. Natl. Acad. Sci. U.S.A. 81*, 7303−7307.
Williams, J. C., Alden, R. G., Murchison, H. A., Peloquin, J. M., Woodbury, N. W., & Allen, J. P. (1992) *Biochemistry 31*, 11029−11037.
Woodbury, N. W. T., & Parson, W. W. (1984) *Biochim. Biophys. Acta 767*, 345−361.
Woodbury, N. W., & Parson, W. W. (1986) *Biochim. Biophys. Acta 850*, 197−210.
Woodbury, N. W., & Allen, J. P. (1995) in *Anoxygenic Photosynthetic Bacteria* (Blankenship, R. E., Madigan, M. T., & Bauer,C. E., Eds.) pp 527−557, Kluwer Academic Publishers, Dordrecht, Netherlands.
Woodbury, N. W., Lin, S., Lin, X., Peloquin, J. M., Taguchi, A. K. W., Williams, J. C., & Allen, J. P. (1995) *Chem. Phys. 197*, 405−421.
Xiao, W., Lin, S., Taguchi, A. K. W., & Woodbury, N. W. (1994) *Biochemistry 33*, 8313−8322.
Yeates, T. O., Komiya, H., Chirino, A., Rees, D. C., Allen, J. P., & Feher, G. (1988) *Proc. Natl. Acad. Sci. U.S.A. 85*, 7993−7997.
Young, D. A., & Marrs, B. L. (1990) *Bot. Mag., Tokyo, Spec. Issue 2*, 3−10.
Youvan, D. C., Ismail, S., & Bylina, E. J. (1985) *Gene 38*, 19−30.
Zilsel, J., Lilburn, T. G., & Beatty, J. T. (1989) *FEBS Lett. 253*, 247−252.
Zinth, W., & Kaiser, W. (1993) in *The Photosynthetic Reaction Center* (Deisenhofer, J., & Norris, J. R., Eds.) Vol. 2, pp 71, Academic Press, San Diego, CA.

BI9521957